CHEMISTRY OF MATERIALS
Article

Chem. Mater. **2009,** *21,* 2851–2861 2851
DOI:10.1021/cm900635u

Tunable Photoluminescence of Ag Nanocrystals in Multiple-Sensitive Hybrid Microgels

Weitai Wu, Ting Zhou, and Shuiqin Zhou*

Department of Chemistry and The Center for Engineered Polymeric Materials of College of Staten Island and The Graduate Center, The City University of New York, 2800 Victory Boulevard, Staten Island, New York 10314

Received March 5, 2009. Revised Manuscript Received April 21, 2009

We report here fluorescent pH-sensitive hybrid materials based on the in situ immobilization of Ag and Ag/Au bimetallic nanoparticles (NPs) in the interior of multiple sensitive copolymer microgels of poly(*N*-isopropylacrylamide-co-acrylic acid-co-acrylamide) with polyacrylamide fragments serving as stabilizing ligands. Temperatures corresponding to the swollen, partially swollen, and nearly collapsed states of the template microgels were respectively applied for loading and in situ chemical reduction of Ag^+ ions to control the size and size distribution of the Ag NPs in the microgels. Au nanoclusters were stably grown on the surface of Ag NPs through a galvanic replacement reaction between Ag and $AuCl_4^-$. The pH-sensitive optical properties of hybrid microgels embedded with either Ag NPs or Ag/Au bimetallic NPs were systematically investigated. The gradual protonization of poly(acrylic acid) fragments shrank the microgels, resulting in an enhancement of photoluminescence (PL) intensity and a blue shift of the emission maximum of the Ag NPs. The surface modification of small Ag NPs with Au nanoclusters reduced the pH sensitivity of PL property changes but dramatically enhanced the PL signals in the near-infrared regime of the hybrid microgels. The method presented here opens a new door in the synthesis of materials with pH-responsive optical properties for biomedical applications.

Introduction

Responsive hybrid materials, based on inorganic nanoparticles (NPs) immobilized in smart polymer carriers, have recently attracted intensive interest.[1−13] While inorganic NPs exhibit size-, shape-, and interdistance-dependent optical, magnetic, electronic, and catalytic properties,[14−16] smart polymers can undergo a volume phase transition in response to external stimuli, such as temperature,[17] pH,[18] or light,[19] to modify the physicochemical environment of the components immobilized inside. Thus, the hybrid materials with inorganic NPs embedded in smart polymers, combining the properties from both inorganic NPs and responsive polymers, can offer possibilities for external switching and manipulation when applied to sensors, electronic/optical devices, and catalytic reactions.

Materials with pH-responsive optical properties are becoming more and more important for the investigation of diseases such as cancer and cystic fibrosis that are associated

*To whom correspondence should be addressed. Tel.: 718-982-3897. E-mail: zhoush@mail.csi.cuny.edu.

(1) (a) Zhang, J.; Xu, S.; Kumacheva, E. *J. Am. Chem. Soc.* **2004**, *126*, 7908. (b) Zhang, J.; Xu, S.; Kumacheva, E. *Adv. Mater.* **2005**, *17*, 2336. (c) Das, M.; Sanson, N.; Kumacheva, E. *Chem. Mater.* **2008**, *20*, 7157.
(2) Tokareva, I.; Minko, S.; Fendler, J. H.; Hutter, E. *J. Am. Chem. Soc.* **2004**, *126*, 15950.
(3) (a) Pich, A.; Bhattacharya, S.; Lu, Y.; Boyko, V.; Adler, H. J. *Langmuir* **2004**, *20*, 10706. (b) Pich, A.; Karak, A.; Lu, Y.; Ghosh, A. K.; Adler, H. J. *Macromol. Rapid Commun.* **2006**, *27*, 344.
(4) Gong, Y.; Gao, M.; Wang, D.; Mohwald, H. *Chem. Mater.* **2005**, *17*, 2648.
(5) Li, J.; Hong, X.; Liu, Y.; Li, D.; Wang, Y.; Li, J.; Bai, Y.; Li, T. *Adv. Mater.* **2005**, *17*, 163.
(6) Xu, H.; Xu, J.; Zhu, Z.; Liu, H.; Liu, S. *Macromolecules* **2006**, *39*, 8451.
(7) (a) Suzuki, D.; Kawaguchi, H. *Langmuir* **2005**, *21*, 8175. (b) Suzuki, D.; Kawaguchi, H. *Langmuir* **2006**, *22*, 3818.
(8) (a) Lu, Y.; Mei, Y.; Drechsler, M.; Ballauff, M. *Angew. Chem., Int. Ed. Engl.* **2006**, *45*, 813. (b) Lu, Y.; Mei, Y.; Schrinner, M.; Ballauff, M.; Moller, M. W.; Breu, J. *J. Phys. Chem. C* **2007**, *111*, 7676.
(9) Palioura, D.; Armes, S. P.; Anastasiadis, S. H.; Vamvakaki, M. *Langmuir* **2007**, *23*, 5761.
(10) (a) Karg, M.; Lu, Y.; Carbo-Argibay, E.; Pastoriza-Santos, I.; Perez-Juste, J.; Liz-Marzán, L.; Hellweg, T. *Langmuir* **2009**, *25*, 3163. (b) Contreras-Caceres, R.; Sanchez-Iglesias, A.; Karg, M.; Pastoriza-Santos, I.; Perez-Juste, J.; Pacifico, J.; Hellweg, T.; Fernandez-Barbero, A.; Liz-Marzán, L. *Adv. Mater.* **2008**, *20*, 1666. (c) Karg, M.; Pastoriza-Santos, I.; Liz-Marzán, L.; Hellweg, T. *Chem. Phys. Chem* **2006**, *7*, 2298.
(11) Agrawal, M.; Rubio-Retama, J.; Zafeiropoulos, N. E.; Gaponik, N.; Gupta, S.; Cimrova, V.; Lesnyak, V.; López-Cabarcos, E.; Tzavalas, S.; Rojas-Reyna, R.; Eychmller, A.; Stamm, M. *Langmuir* **2008**, *24*, 9820.
(12) Gupta, S.; Uhlmann, P.; Agrawal, M.; Chapuis, S.; Oertel, U.; Stamm, M. *Macromolecules* **2008**, *41*, 2874.
(13) Cheng, Z.; Liu, S.; Beines, P. W.; Ding, N.; Jakubowicz, P.; Knoll, W. *Chem. Mater.* **2008**, *20*, 7215.
(14) (a) Murray, C. B.; Norris, D. J.; Bawendi, M. G. *J. Am. Chem. Soc.* **1993**, *115*, 8706. (b) Redl, F. X.; Black, C. T.; Papaefthymiou, G. C.; Sandstrom, R. L.; Yin, M.; Zeng, H.; Murray, C. B.; O'Brien, S. P. *J. Am. Chem. Soc.* **2004**, *126*, 14583.
(15) (a) Chan, W. C. W.; Nie, S. *Science* **1998**, *281*, 2016. (b) Sun, Y. G.; Xia, Y. *Science* **2002**, *298*, 2176.
(16) (a) Zhong, C. J.; Maye, M. M.; Luo, J.; Han, L.; Kariuki, N. N. Nanoparticles in Catalysis. In Nanoparticles: Building Blocks for Nanotechnology; Rotello, V. M., Ed.; Kluwer Academic Publishers: Dordrecht, the Netherlands, **2004**; pp 113−144.(b) Njoki, N.; Lim, S. I.-I.; Mott, D.; Park, H. Y.; Khan, B.; Mishra, S.; Sujakumar, R.; Luo, J.; Zhong, C. J. J. Phys. Chem. C **2007**, 111, 14664.
(17) (a) Schild, H. G. *Prog. Polym. Sci.* **1992**, *17*, 163. (b) Wu, C.; Zhou, S. Q. *Macromolecules* **1995**, *28*, 8381.(c) 1997, *30*, 574.
(18) (a) Zhou, S. Q.; Chu, B. *J. Phys. Chem. B* **1998**, *102*, 1364. (b) Ito, S.; Ogawa, K.; Suzuki, H.; Wang, B.; Yoshida, R.; Kokufuta, E. *Langmuir* **1999**, *15*, 4289. (c) Hoare, T.; Pelton, R. *Macromolecules* **2004**, *37*, 2544. (d) Hoare, T.; Pelton, R. *Langmuir* **2004**, *20*, 2123.
(19) Gorelikov, I.; Field, L. M.; Kumacheva, E. *J. Am. Chem. Soc.* **2004**, *126*, 15938.

Published on Web 05/18/2009

with disruptions in acid/base homeostasis.[20−23] Immobilization of inorganic NPs in pH-sensitive polymers is one way to make materials with pH-responsive optical properties. Ionov et al.[24] reported the fabrication of nanosensors based on the CdSe NPs immobilized on pH-responsive poly(2-vinyl pyridine) (P2VP) brushes. Similarly, Tokareva et al.[2] and Gupta et al.[12] have immobilized the Au and Ag NPs onto the P2VP brushes, respectively. The pH-induced shrinkage of P2VP chains caused a red shift of the surface plasmon resonance bands of Au and Ag NPs. Kozlovskaya et al.[25] have made pH-responsive ultrathin membranes via postinclusion of Au nanorods into the cross-linked poly(methacrylic acid) (PMAA) hydrogels. The pH-induced shrinkage of the PMAA hydrogel caused a blue shift by 21 nm of the plasmon bands of Au nanorods. Karg et al.[10a] have recently observed a strong red shift of the surface plasmon bands of Au nanorods when assembled on the surface of microgels experiencing a pH-induced collapse. The shrinkage of the template polymers brought the inorganic NPs closer and thus increased the interactions of adjacent NPs to induce a change in optical properties.

Microgels offer several advantages over other polymer template systems to immobilize inorganic NPs: simple synthesis, easy functionalization, uniform size distribution, tunable dimensions, potential biocompatibility, and a very short response time.[1,26,27] Different methods have been recently developed to immobilize inorganic NPs into thermosensitive microgels based on poly(*N*-isopropylacrylamide) (PNIPAM) and its derivatives. Gong et al.[4] incorporated the CdTe NPs into the PNIPAM microgels through the hydrogen bonding between the ligands capped on the CdTe NPs with the PNIPAM chains. Agrawal et al.[11] covered the PNIPAM microgels with the CdTe NPs through the covalent bonding between the ligands capped on the CdTe NPs and the surface functional groups of the microgels. Liz-Marzán et al.[10b,10c] synthesized the PNIPAM microgel shell on the surfactant-capped gold NPs, as well as gold nanorods on the surface of poly(N-isopropylacrylamide-allylacetic acid) microgel, to form core−shell structured hybrid materials. All of these methods require presynthesized inorganic NPs capped with functional ligands. A simple and facile method is in situ template synthesis of inorganic NPs. Kumacheva's group[1a] first developed an in situ template method to synthesize CdS, Fe_3O_4, and Ag NPs randomly distributed in the interior of PNIPAM-based microgels. Using the same in situ template method, Suzuki and Kawaguchi synthesized the Au NPs in the PNIPAM microgels.[7] The temperature-tunable photoluminescence (PL) of CdTe or CdS nanocrystals,[1a,4,5,11] and the UV−visible absorbance of Au NPs,[7,10] have been observed in these hybrid materials. However, few studies have been reported for pH-responsive optical property changes of inorganic NPs immobilized in microgel templates. Kumacheva's group[1a,1b] synthesized Ag NPs in the pH-responsive microgels of poly(N-isopropylacrylamide-acrylic acid-2-hydroxyethyl acrylate) (p(NIPAM-AA-HEA)). The Ag^+ ions were sequestered into the microgels through interaction with the ionized $-COO^-$ groups in AA units. The different ionization degree of AA units at different pH values resulted in different loadings of Ag^+ ions and different swelling extents of microgels, producing Ag NPs with various PL intensities and emission wavelengths. At pH ≥ 8.89, the Ag^+ ions formed a nonfluorescent precipitate of AgOH. However, they found that only the Ag NPs prepared from the photoreduction of Ag^+ ions under UV irradiation were fluorescent, while the Ag NPs prepared from the conventional reduction of Ag^+ ions with a reducing agent were nonfluorescent.

In this work, we present the in situ synthesis of Ag NPs and Ag/Au bimetallic NPs inside a copolymer microgel of poly(N-isopropylacrylamide-acrylic acid-acrylamide) [p(NIPAM-AA-AAm)] using conventional $NaBH_4$ reduction of Ag^+ ions at different temperatures. The pH-responsive optical property changes of the resulted hybrid microgels were systematically studied. The novelty of our work is multiple. First, the polyacrylamide (pAAm) segment is designed to complex with Ag^+ ions for the uptake of Ag^+ precursors and to stabilize the Ag NPs in the microgels.[28] Second, the pNIPAM component in the microgels is used to induce temperature-responsive volume phase transition to control the mesh size and environment of polymer networks for the synthesis of Ag NPs, thus producing different sizes and size distributions of Ag NPs, resulting in different optical properties. Third, the microgels loaded with Ag^+ ions were dialyzed against an acidic solution of pH = 3.8 before the reduction of Ag^+ ions. At pH = 3.8, the AA segments have few ionized $-COO^-$ groups for the uptake of Ag^+ ions. The main function of the AA fragments is used to induce a pH-sensitive volume phase transition of the microgels after the immobilization of Ag NPs, which enables us to systematically study the pH-responsive optical property change of the resulted hybrid microgels. Our results indicated that the Ag NPs synthesized in the swollen microgels at low temperatures have a larger size and a broader size distribution, while the Ag NPs synthesized in the collapsed microgels at a high temperature have a smaller size. Interestingly, all of the Ag NPs synthesized in our p(NIPAM-AA-AAm) microgels from the chemical $NaBH_4$ reduction of Ag^+ ions

(20) Tomasulo, M.; Yildiz, I.; Raymo, F. M. *J. Phys. Chem. B* **2006**, *110*, 3853.
(21) Kim, S.; Pudavar, H. E.; Prasad, P. N. *Chem. Commun.* **2006**, *19*, 2071.
(22) Gilles, R. J.; Raghunand, N.; Carcia-Martin, M. L.; Gatenby, R. A. *IEEE Eng. Med. Biol. Mag.* **2004**, *23*, 57.
(23) Coakley, R. D.; Grubb, B. R.; Paradiso, A. M.; Gatzy, J. T.; Johnson, L. G.; Kreda, S. M.; O'Neal, W. K.; Boucher, R. C. *Proc. Natl. Acad. Sci. U. S. A.* **2003**, *100*, 16083.
(24) Ionov, L.; Sapra, S.; Synytska, A.; Rogach, A. L.; Stamm, M.; Diez, S. *Adv. Mater.* **2006**, *18*, 1453.
(25) Kozlovskaya, V.; Kharlampieva, E.; Khanal, B. P.; Manna, P.; Zubarev, E. R.; Tsukruk, V. V. *Chem. Mater.* **2008**, *20*, 7474.
(26) Reese, C. E.; Mikhonin, A. V.; Kamenjicki, M.; Tikhonov, A.; Asher, S. A. *J. Am. Chem. Soc.* **2004**, *126*, 1493.
(27) Zhang, Y.; Guan, Y.; Zhou, S. *Biomacromolecules* **2007**, *8*, 3842.
(28) (a) Yez-Sedeo, P.; Pingarrn, J. M. *Anal. Bioanal. Chem.* **2005**, *382*, 884. (b) Xiong, Y. J.; Siekkinen, A. R.; Wang, J. G.; Yin, Y. D.; Kim, M. J.; Xia, Y. N. *J. Mater. Chem.* **2007**, *17*, 2600.

are fluorescent. The pH-induced shrinkage of the microgels systematically enhanced the PL intensity and caused a blue shift of the emission wavelength. These results are different from the previously reported nonfluorescent Ag NPs synthesized from the chemical reduction of Ag^+ ions in a different type of microgel.[1b] In addition, Au nanoclusters could be stably grown on the surface of Ag NPs immobilized in the microgels by a galvanic replacement reaction between Ag and $AuCl_4^-$.[29] The hybrid microgels with Au/Ag bimetallic NPs immobilized inside still exhibit pH-sensitive PL. Furthermore, the surface modification of Ag NPs with Au nanoclusters significantly enhances the near-infrared (wavelength 800−900 nm) PL intensity of the resulted hybrid microgels. The hybrid microgels presented in this study may find important applications in biosensor and bioimage technology for early diagnosis and therapy of diseases.[30−32]

Experimental Section

Materials. All chemicals were purchased from Aldrich. NIPAM was recrystallized from a hexane−toluene (a 1:1 volume ratio) mixture and dried in a vacuum. AA was purified by distillation under reduced pressure to remove inhibitors. Silver nitrate ($AgNO_3$), chloroauric acid trihydrate ($HAuCl_4 \cdot 3H_2O$), sodium borohydrate ($NaBH_4$), L-ascorbic acid, AAm, *N*, *N*′-methylenebisacrylamide (MBAAm), ammonium persulfate (APS), and sodium dodecyl sulfate (SDS) were used as received without further purification. The water used in all experiments was of Millipore Milli-Q grade.

Microgel Synthesis. The microgels were prepared by free radical precipitation copolymerization of NIPAM, AAm, AA, and MBAAm using APS as an initiator. A mixture of NIPAM (1.405 g), AAm (0.091 g), AA (0.061 g), MBAAm (0.101 g), SDS (0.050 g), and water (95 mL) was poured into a 250 mL three-neck round-bottom flask equipped with a stirrer, a nitrogen gas inlet, and a condenser. The mixture was heated to 70 °C under a N_2 purge. After 30 min, 5 mL of 0.089 M APS was added to initiate the polymerization. The reaction was allowed to proceed for 5 h. The obtained p(NIPAM-AA-AAm) copolymer microgels were purified by centrifugation (Thermo Electron Co. SORVALL RC-6 PLUS superspeed centrifuge) and decantation and then washed with water. The resultant microgel was further purified by 3 days of dialysis (Spectra/Por molecularporous membrane tubing, cutoff 12 000−14 000, the same below) against very frequently changed water at room temperature (~22 °C).

In Situ Synthesis of Ag NPs in p(NIPAM-AA-AAm) Microgels. A series of hybrid microgels with Ag NPs immobilized inside were synthesized from the same p(NIPAM-AA-AAm) microgels but dispersed at three different temperatures of 22 °C, 38 °C, and 43 °C. Typically, the mixture of 0.201 g $AgNO_3$ with 45.775 g p(NIPAM-AA-AAm) microgel suspensions was stirred at a designed temperature for 4 h in a 100 mL round-bottom flask under a N_2 purge. After that, excess $AgNO_3$ was removed at the same designed temperature by centrifugation, decantation, and dialysis against water of pH ≈ 3.8 and then washed with water until the dispersion had a neutral pH. The microgels loaded with Ag^+ ions were poured into a 250 mL round-bottom flask equipped with a stirrer, a nitrogen gas inlet, and a condenser and maintained at the same designed temperature. After a 30 min N_2 purge, a $NaBH_4$ solution (0.44 g in 5 mL water) was added dropwise. The mixture was further stirred for 50 min. The resulted microgels incorporated with Ag NPs were then purified by centrifugation, decantation, and 1 h of dialysis against very frequently changed water at the same designed temperature. Finally, the hybrid microgels were dialyzed against water at room temperature for another 16 h. The obtained hybrid microgels were coded as p(NIPAM-AA-AAm)-Ag.

In Situ Synthesis of Au/Ag Bimetallic NPs in the p(NIPAM-AA-AAm) Microgels. Au/Ag bimetallic NPs in the microgels were prepared using the galvanic replacement reaction.[7,28,29] A mixture of p(NIPAM-AA-AAm)-Ag hybrid microgels (5.0 mL) and water (15.0 mL) in a 50 mL glass vial was stirred in an ice water bath for 30 min, a solution of $HAuCl_4$ (1.0 wt %, 400 μL) was then added dropwise to the vial. The immediate color change revealed the galvanic replacement reaction between Ag and Au(III). The solution was stirred for another 20 min until the color was stable. After that, a solution of L-ascorbic acid (100 mM, 800 μL) was added dropwise to allow the seed-mediated growth of Au nanoclusters. The reaction was continued for 18 min. The final hybrid microgels with Au/Ag bimetallic NPs incorporated were purified by centrifugation, decantation, and dialysis against water at room temperature. The hybrid microgels were coded as p(NIPAM-AA-AAm)-Ag/Au.

Characterization. The FTIR spectra of the dried microgels were recorded with a Nicolet Instrument Co. MAGNA-IR 750 Fourier transform infrared spectrometer. The UV−vis absorption spectra were obtained on a Thermo Electron Co. Helios β UV−vis spectrometer. The PL spectra of the hybrid microgel dispersions at different pH values were obtained on a JOBIN YVON Co. FluoroMax-3 spectrofluorometer equipped with a Hamamatsu R928P photomultiplier tube, a calibrated photodiode for excitation reference correction from 200 to 980 nm, and an integration time of 1 s. The R298P detector can be used for photon counting for the UV to near IR range in a typical spectral response range of 185−900 nm. The detector has high sensitivity at 185−850 nm but plummets precipitously in sensitivity beyond 850 nm. To confirm the near-IR emissions, the PL spectra were also recorded on a VARIAN CARY Eclipse Fluorescence spectrophotometer equipped with an R928 photomultiplier tube and self-optimized light filters. The pH values were obtained on a Mettler Toledo SevenEasy pH meter. The transmission electron microscopy (TEM) images were taken on an FEI TECNAI transmission electron microscope at an accelerating voltage of 120 kV. Approximately 10 μL of the diluted microgel suspension was air-dried on a carbon-coated copper grid for the TEM measurements.

Dynamic light scattering (DLS) was performed on a standard laser light scattering spectrometer (BI-200SM) equipped with a BI-9000 AT digital time correlator (Brookhaven Instruments, Inc.). A Nd:YAG laser (150 mW, 532 nm) was used as the light source. All microgel solutions were passed through Millipore Millex-HV filters with a pore size of 0.80 μm to remove dust before the DLS measurements. In DLS, the Laplace inversion of each measured intensity−intensity time-correlated function can result in a characteristic line width distribution $G(\Gamma)$.[33] For a

(29) Au, L.; Lu, X. M.; Xia, Y. N. *Adv. Mater.* **2008**, *20*, 2517.
(30) (a) Hirsch, L. R.; Stafford, R. J.; Bankson, J. A.; Sershen, S. R.; Rivera, B.; Price, R. E.; Hazle, J. D.; Halas, N. J.; West, J. L. *Proc. Natl. Acad. Sci. U. S. A.* **2003**, *100*, 13549. (b) Cognet, L.; Tardin, C.; Boyer, D.; Choquet, D.; Tamarat, P.; Lounis, B. *Proc. Natl. Acad. Sci. U. S. A.* **2003**, *100*, 11350.
(31) (a) El-Sayed, I. H.; Huang, X.; El-Sayed, M. A. *Nano Lett.* **2005**, *5*, 829. (b) El-Sayed, I. H.; Huang, X.; El-Sayed, M. A. *Cancer Lett.* **2006**, *239*(1), 129.
(32) Hilderbrand, S. A.; Kelly, K. A.; Niedre, M.; Weissleder, R. *Bioconjugate Chem.* **2008**, *19*, 1635.
(33) Chu, B. Laser Light Scattering, 2nd ed.; Academic Press: New York, 1991.

purely diffusive relaxation, Γ is related to the translational diffusion coefficient D by $(\Gamma/q^2)_{C\rightarrow 0,q\rightarrow 0} = D$, where $q = (4\pi n/\lambda)\sin(\theta/2)$ with n, λ, and θ being the solvent refractive index, the wavelength of the incident light in vacuo, and the scattering angle, respectively. $G(\Gamma)$ can be further converted to a hydrodynamic radius (R_h) distribution by using the Stokes−Einstein equation, $R_h = (k_B T/6\pi\eta)D^{-1}$, where T, k_B, and η are the absolute temperature, the Boltzmann constant, and the solvent viscosity, respectively.

Results and Discussion

Synthesis of p(NIPAM-AA-AAm) Microgels. The multiple-sensitive p(NIPAM-AA-AAm) microgels were synthesized from the free radical precipitation copolymerization of NIPAM, AAm (8.4 mol %), and AA (5.6 mol %) using MBAAm (4.3 mol %) as a cross-linker. The preparation of nearly monodispersed p(NIPAM-AA) microgels and p(NIPAM-AAm) microgels in water with controllable sizes and compositions has been well-established.[18] It has been reported that the contents of functional monomer AA or AAm in the pNIPAM-based microgels are nearly equal to their feeding compositions.[18c] In our present p(NIPAM-AA-AAm) microgels, the content of AA units determined from titration was 5.4 mol % (~4% lower than the feed). The FTIR spectrum of the p(NIPAM-AA-AAm) microgels shows the characteristic absorptions including amide I at 1650 cm^{-1}, amide II at 1538 cm^{-1}, and the stretching of the uncharged dimerized or associated form of −COOH groups in AA units at 1710 cm^{-1}.

Volume Phase Transitions of p(NIPAM-AA-AAm) Microgels. Figure 1 shows the temperature-induced volume phase transitions of the p(NIPAM-AA-AAm) microgels dispersed at pH = 3.78 and 6.65, in terms of the change of R_h measured at a scattering angle of $\theta = 45°$. The pH of microgel dispersions was adjusted by using dilute HCl or NaOH aqueous solutions. The pK_a value of the AA moiety in the p(NIPAM-AA) microgels is about 4.2.[34] At pH = 6.65, AA groups are totally deprotonated, resulting in an increase in osmotic pressure and Coulombic repulsion for full swelling of the microgels. In addition, the AAm fragments are also very hydrophilic. To induce the p(NIPAM-AA-AAm) chain to collapse, a higher temperature needs to be provided. No volume phase transition was detected in our experimental temperature window (<47.5 °C). The microgels only gradually shrank down 10% in the R_h value when the temperature was increased from 22 to 47.5 °C. At pH = 3.78, AA groups are protonated, and the size of the microgels is significantly reduced in comparison with the ionized microgels at pH = 6.65. The 10 mol % neutral AA fragments have little effect on the volume phase transition temperature of p(NIPAM-AA) microgels compared to pure pNIPAM microgels.[35] However, the 10.6 mol % hydrophilic AAm fragments enhanced the volume phase transition temperature of our p(NIPAM-AA-AAm) microgels. A two-step volume phase transition with a swelling ratio of R_h(22 °C)/R_h(45 °C) = 1.86

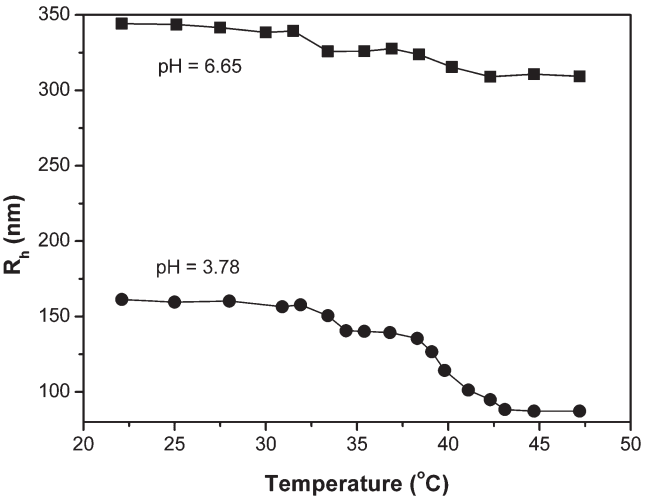

Figure 1. Average R_h value of the p(NIPAM-AA-AAm) microgels as a function of the temperature, measured at a scattering angle $\theta = 45°$ and pH = 3.78 and pH = 6.65.

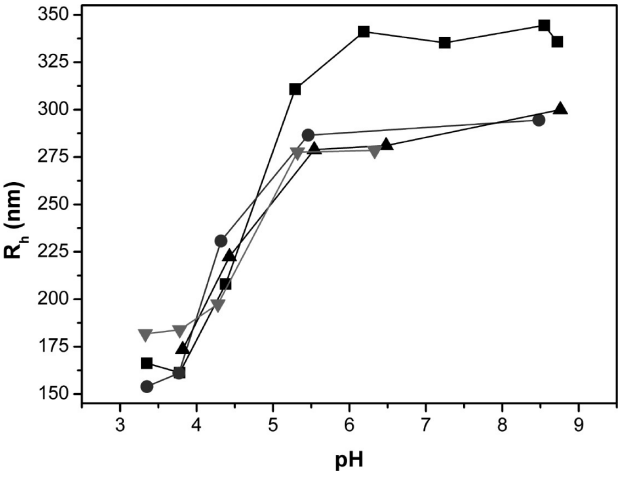

Figure 2. pH dependence of the average R_h value of the p(NIPAM-AA-AAm) template microgels (■) and the p(NIPAM-AA-AAm)-Ag hybrid microgels synthesized at different temperatures of 22 °C (●), 38 °C (▲), and 43 °C (▼), measured at 22.1 °C and a scattering angle $\theta = 45°$.

was observed. The broad volume phase transition of the p(NIPAM-AA-AAm) microgels at pH = 3.78 could be attributed to the cross-linker heterogeneity[17,35] and the hydrogen-bonding complexation of the amide group in the AAm fragments with the protonated COOH groups in AA units. Nevertheless, the temperature-responsive volume phase transition of the p(NIPAM-AA-AAm) microgels allows us to control the mesh size and the hydrophilicity/hydrophobicity environment of the polymer network for the in situ synthesis of Ag NPs.

Figure 2 shows the pH-induced volume phase transition of the p(NIPAM-AA-AAm) microgels in terms of the change of R_h measured at $T = 22.1$ °C and a scattering angle of $\theta = 45°$. As expected, the functional AA segments on the copolymer chains of microgels resulted in a pH-responsive volume phase transition. At pH values below the pK_a of AA, the size of the microgels remained nearly constant. When the pH was over the pK_a of AA, the AA groups were gradually deprotonated. The Coulombic repulsion among the ionized carboxylate groups increased the osmotic pressure, resulting in a gradual

(34) Cesarano, J.; Aksay, I. A.; Bleier, A. *J. Am. Ceram. Soc.* **1988**, *71*, 250.
(35) Jones, C. D.; Lyon, L. A. *Macromolecules* **2003**, *36*, 1988.

increase in the size of microgels until all AA groups were deprotonated at pH > 5.5, where the microgels reached a maximum swelling ratio R_h(charged)/R_h(uncharged) of 2.2. The pH-responsive volume phase transition of the p(NIPAM-AA-AAm) microgels allows us to change the interactions of the Ag or Au/Ag NPs immobilized inside the polymer networks and their local surface environments.

In Situ Synthesis of p(NIPAM-AA-AAm)-Ag Microgels. It should be noted that the p(NIPAM-AA-AAm) microgels could undergo a complete volume phase transition when the temperature was increased from 22 to 45 °C at pH = 3.78 (see Figure 1). Here, we have chosen three different temperatures of 22 °C, 38 °C, and 43 °C, corresponding to the swollen, partially swollen, and nearly fully collapsed state of microgels, respectively, for the uptake and reduction of Ag^+ ions to immobilize the Ag NPs inside the microgels. The different mesh size and environment of the polymer network at these temperatures are used to control the size and size distribution of Ag NPs. Both carboxylate groups and amino groups are able to link metal ions/nanoparticles.[28] Our motivation is to use the amino groups in the AAm units to complex the Ag^+ ions into the microgels from the external $AgNO_3$ solution and to protect the reduced Ag NPs from agglomeration or release. After the uptake of Ag^+ ions into the microgels, the excess $AgNO_3$ in the external solution was removed by centrifugation, decantation, and dialysis against a dilute HCl solution of pH = 3.8 at a designed temperature. This procedure is designed not only to ensure that Ag NPs can only be formed inside the microgels but also to ensure that most of Ag^+ ions are loaded into the microgels through the coordination between the Ag^+ ions and the amino groups in AAm segments because the AA segments have little ionized COO^- groups for the uptake of Ag^+ ions at pH = 3.8. In such a design, the carboxylic acid groups in AA segments are mainly used to induce a pH-responsive volume phase transition of the microgels after the immobilization of Ag NPs stabilized with amino groups in AAm segments. The incorporation of the Ag NPs into the microgels almost has no effect on the characteristic absorption peaks of carboxylic acid, amide I, and amide II groups in FTIR spectra. However, the incorporation of Ag NPs into the microgels slightly reduced the swelling degree of the microgels. As shown in Figure 2, the sizes of the p(NIPAM-AA-AAm) microgels and the p(NIPAM-AA-AAm)-Ag hybrid microgels are nearly the same at the shrunken state (pH < 3.8), while the size of all of the p(NIPAM-AA-AAm)-Ag hybrid microgels is smaller than that of p(NIPAM-AA-AAm) microgels at the fully swollen state after the ionization of AA groups. The size decrease of the p(NIPAM-AA-AAm)-Ag hybrid microgels in the swollen state could be associated with an increase in the cross-linking degree of the gel networks. The Ag NPs can act as cross-linking points when they are stabilized inside the gel networks through the linkages with the amino groups of AAm segments. A similar size decrease in the swollen state was also observed when the CdTe nanocrystals were incorporated into the PNIPAM microgels.[4] The obtained p(NIPAM-AA-AAm)-Ag hybrid microgels were very stable. No sediment was observed after 3 months' placement at room temperature. The Ag NPs were not released from the microgel even at the most swollen state (pH ≈ 6, dialysis in ice water for 10 h) due to the strong interaction of Ag NPs with the amino groups of AAm fragments and the ionized carboxylate groups of AA units. It should be mentioned that the different swelling degrees (or mesh size) of the template microgels at different pH values could be also used to control the size of the Ag NPs. At pH > 6, both the amino groups in AAm units and the ionized COO^- groups in AA units can sequester the Ag^+ ion precursors into the fully swollen microgels. The in situ reduction of these Ag^+ ions will result in a larger loading and size of Ag NPs. However, we found that the Ag NPs immobilized through the COO^- groups in AA units became unstable and easily released from the microgels when the pH was decreased to below 4.2, where the COO^- groups in AA units became COOH groups and could not stabilize the Ag NPs effectively. These systems are not suitable for the systematic study of the pH-responsive optical property because the Ag NPs embedded in the microgels could be partially released at low pH values.

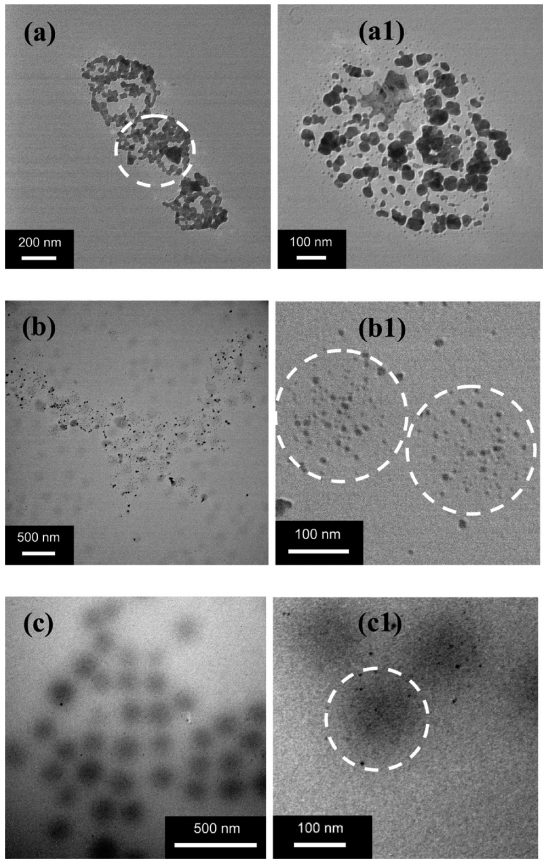

Figure 3. TEM images of the p(NIPAM-AA-AAm)-Ag hybrid microgels synthesized from the p(NIPAM-AA-AAm) template microgels dispersed at 22 °C (a), 38 °C (b), and 43 °C (c).

Figure 3 shows the TEM images of the p(NIPAM-AA-AAm)-Ag hybrid microgels synthesized at temperatures of 22 °C, 38 °C, and 43 °C. At 22 °C, the polymer network is swollen at pH = 3.8; the in situ reduction of the loaded

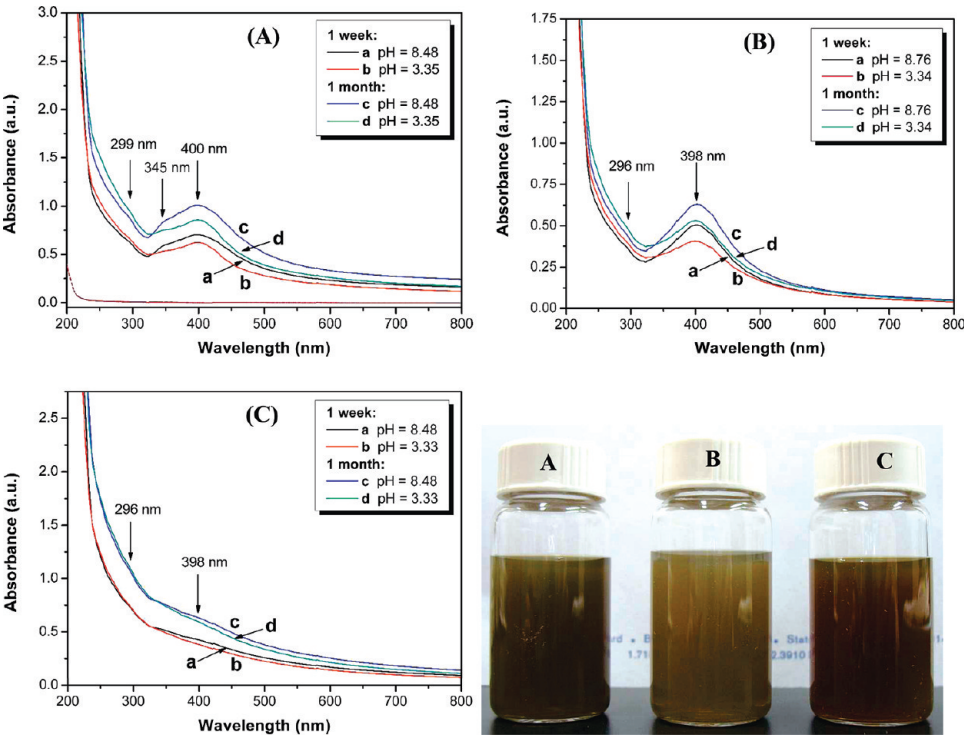

Figure 4. UV−vis absorbance spectra of the p(NIPAM-AA-AAm)-Ag hybrid microgels synthesized from the p(NIPAM-AA-AAm) template microgels dispersed at 22 °C (A), 38 °C (B), and 43 °C (C). The p(NIPAM-AA-AAm) microgels show no absorbance in the range of 220−800 nm (dash line in A). The photograph presents the color for the dispersion of each hybrid microgel at room temperature.

Ag^+ ions in the open network resulted in large Ag NPs with a broad size distribution. When the dimension of the microgels shrank down to about 70% of its swollen size at 38 °C, the in situ reduced Ag NPs had a much smaller size with a more uniform size distribution. When the template microgels collapsed nearly completely at 43 °C, the mesh size was very small, which resulted in very small size of Ag NPs confined inside the microgels. Clearly, the temperature-controllable mesh size of the template microgels is important for us to in situ immobilize the Ag NPs with different sizes and size distributions.

In Situ Synthesis of Au/Ag Bimetallic NPs in the p(NIPAM-AA-AAm) Microgels. The p(NIPAM-AA-AAm)-Ag/Au hybrid microgels were prepared through the titration of the template p(NIPAM-AA-AAm)-Ag hybrid microgels with the $AuCl_4^-$ solution. The addition of $AuCl_4^-$ induced an immediate galvanic replacement reaction with Ag NPs, leading to the formation of bimetallic Ag/Au NPs in the interior of the p(NIPAM-AA-AAm) microgels. The feeding ratio of Au(III) to Ag(0) is controlled to be very low, so even a complete galvanic reaction would not result in a complete replacement of the Ag atoms with Au atoms. Briefly, $AuCl_4^-$ oxidizes the sacrificial Ag template to AgCl, which is highly soluble at the reaction temperature, as estimated from its solubility (1.92×10^{-3} g L^{-1} at 25 °C). The standard reduction potential of the $AuCl_4^-$/Au pair (0.99 V) is higher than that of the AgCl/Ag pair (0.22 V). The electrons generated in the oxidation process migrate to the surface of the Ag particles, where they reduce the $AuCl_4^-$ to Au atoms. Because Au and Ag solids share the same face-centered cubic structure with closely matched lattice constants (4.0786 and 4.0862 Å, respectively), the Au atoms are able to epitaxially nucleate and grow on the surface of the Ag particles.[29] Thus, observation of the surface plasmon absorption change of the p(NIPAM-AA-AAm)-Ag/Au hybrid microgels after the surface modification of the Ag NPs in the p(NIPAM-AA-AAm)-Ag hybrid microgels could be expected.

UV−Vis Absorption Properties of p(NIPAM-AA-AAm)-Ag and p(NIPAM-AA-AAm)-Ag/Au Hybrid Microgels. Figure 4 shows the UV−vis absorption spectra of the three p(NIPAM-AA-AAm)-Ag hybrid microgels prepared at 22 °C (A), 38 °C (B), and 43 °C (C), at pH's well below and above the pK_a of AA groups. The samples showed nearly the same absorption profiles after being set for one week and one month at room temperature, indicating that the hybrid microgels were very stable in aqueous solutions. The peak near 400 nm (3.1 eV) is assigned to the surface plasmon absorbance of Ag NPs immobilized in the microgels. The broad peaks located at 296 and 299 nm are attributed to small Ag_n clusters, which is different from the surface plasmon absorption of Ag NPs.[36] The spectra in Figure 4 indicate that the small Ag_n clusters can coexist with the relatively large Ag NPs, which could be ascribed to the "magic-number" phenomenon and odd−even effects in the stability of the small clusters.[37] The shape of the surface plasmon absorption spectrum is determined by the relative

(36) (a) Gaddy, G. A.; McLain, J. L.; Steigerwalt, E. S.; Broughton, R.; Slaten, B. L.; Mills, G. *J. Cluster Sci.* **2001**, *12*, 457. (b) Henglein, A.; Mulvaney, P.; Linnert, T. *Faraday Discuss. Chem. Soc.* **1991**, *92*, 31.

(37) (a) Fayet, P.; Wöste, L. *Surf. Sci.* **1985**, *156*, 134. (b) Henglein, A. *J. Phys. Chem.* **1993**, *97*, 5457. (c) He, P.; Shen, X. H.; Gao, H. C. *Acta Phys. Chim. Sin.* **2004**, *20*(10), 1200.

dimensions of the particle to the wavelength of incident electromagnetic (EM) radiation. When NPs have much smaller dimensions than the wavelength of the incident beam, the EM field across the particles is uniform such that all of the conduction electrons move in-phase, producing only dipole-type oscillations manifested by a single, narrow peak in the spectrum. As the particle size increases, the EM field across the particle becomes nonuniform. This phase retardation broadens the dipole resonance and excites higher multipole resonances, leading to several peaks in the spectra.[38] Figure 4 clearly shows the differences in the surface plasmon absorption bands obtained from the hybrid microgels prepared at different temperatures. The Ag NPs synthesized in the open polymer networks at 22 °C have a large size and a broad size distribution, resulting in a broad and asymmetrical surface plasmon absorption band with a maximum at 400 nm (A). In contrast, the Ag NPs synthesized in the partially shrunken polymer networks at 38 °C have a much smaller size and narrower size distribution, producing a narrower and more symmetrical surface plasmon band with the maximum shifted to higher energy at 398 nm (B). This slight shift could be explained from the "merging" of the particle's surface charge over a smaller surface area so that the surrounding medium poorly compensates the restoring force, thus speeding the electron oscillations. When the Ag NPs were synthesized in the nearly completely collapsed polymer network at 43 °C, the surface plasmon absorption showed a distinct decrease but could still be faintly seen (C). The decreased surface plasmon absorption indicated that the in situ reduced Ag NPs in the collapsed microgels might be mainly presented as the small Ag_n clusters with a small amount of relatively large Ag NPs. The different UV−vis absorption spectra made the three p(NIPAM-AA-AAm)-Ag hybrid microgels display quite different colors, which could be distinguished easily by the naked eye. The poor transparency of the samples in the photographs is due to the high concentrations of hybrid microgels held in large vials. The pH effect on the UV−vis absorption was also examined for all of the p(NIPAM-AA-AAm)-Ag hybrid microgels. The ionization of AA groups in the p(NIPAM-AA-AAm) microgels at pH > pK_a increases the surface plasmon absorption of the relatively large Ag NPs but reduces the higher-energy absorption band of the small Ag_n clusters. These changes were unambiguously associated with the different states of Ag particles at different swelling degrees of the microgels followed by pH adjustment.[7,38]

Figure 5 shows the UV−vis absorption spectra of the p(NIPAM-AA-AAm)-Ag/Au hybrid microgels prepared from the template p(NIPAM-AA-AAm)-Ag hybrid microgels synthesized at 22 °C (a), 38 °C (b), and 43 °C (c). After the surface modification of Ag NPs with the Au atoms, the surface plasmon absorption at about 400 nm from Ag NPs decreased or even disappeared, while the surface plasmon bands above 500 nm from Au nanoclusters appeared. In addition, the surface plasmon bands of the

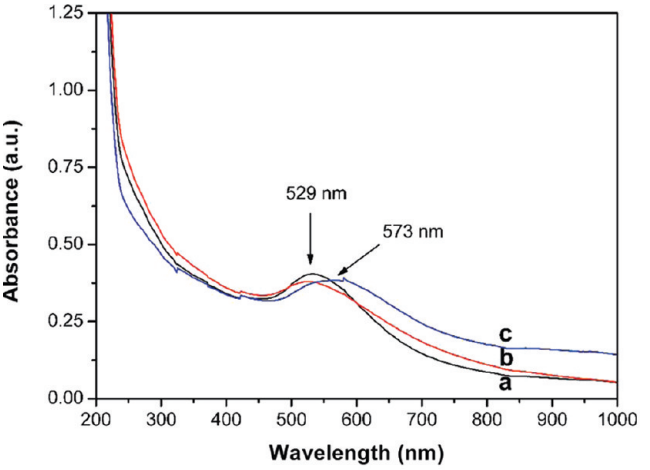

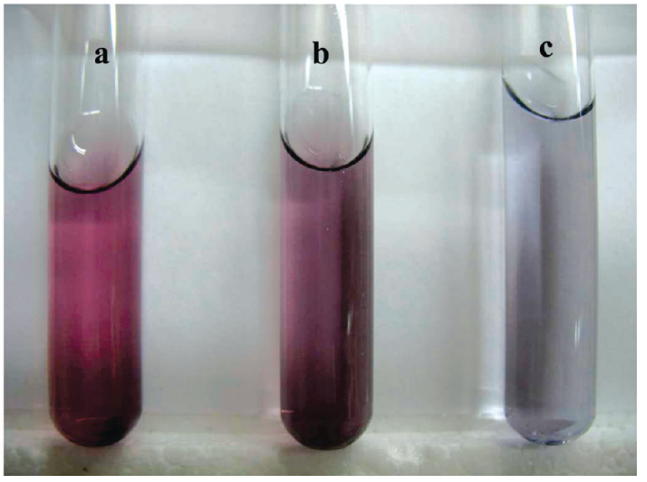

Figure 5. UV−vis absorbance spectra of the p(NIPAM-AA-AAm)-Ag/Au microgels made from the surface modification of Ag NPs with Au nanoclusters in the interior of the p(NIPAM-AA-AAm)-Ag hybrid microgels synthesized at 22 °C (a), 38 °C (b), and 43 °C (c). The photograph presents the color for the dispersion of each hybrid microgel at room temperature.

three p(NIPAM-AA-AAm)-Ag/Au hybrid microgels show different maximum peak positions, resulting in the color changes from red to purple, and then blue, corresponding to the template p(NIPAM-AA-AAm)-Ag hybrid microgels synthesized at 22 °C (a), 38 °C (b), and 43 °C (c). The differences in the absorption spectra of these samples might be due to the different surface characteristics and topologies[39] of the Ag/Au bimetallic NPs as well as the different Ag/Au content ratios in the Ag/Au bimetallic NPs, which would also affect their photoluminescence.

pH-Sensitive PL Property of p(NIPAM-AA-AAm)-Ag and p(NIPAM-AA-AAm)-Ag/Au Hybrid Microgels. The PL spectra for all of the p(NIPAM-AA-AAm)-Ag and p(NIPAM-AA-AAm)-Ag/Au hybrid microgel dispersions at different pH values were collected at room temperature (~22 °C). Two groups of PL peaks in the near-ultraviolet wavelength range of 300−450 nm (Figure 6 and 7) and the visible/near-IR wavelength range of 550−850 nm (Figure 8) were recorded at different excitation wavelengths in the effective spectral range.

(38) Evanoff, D. D.Jr.; Chumanov, G. *Chem. Phys. Chem.* **2005**, *6*, 1221.

(39) Mohamed, M. B.; Volkov, V.; Link, S.; El-Sayed, M. A. *Chem. Phys. Lett.* **2000**, *317*, 517.

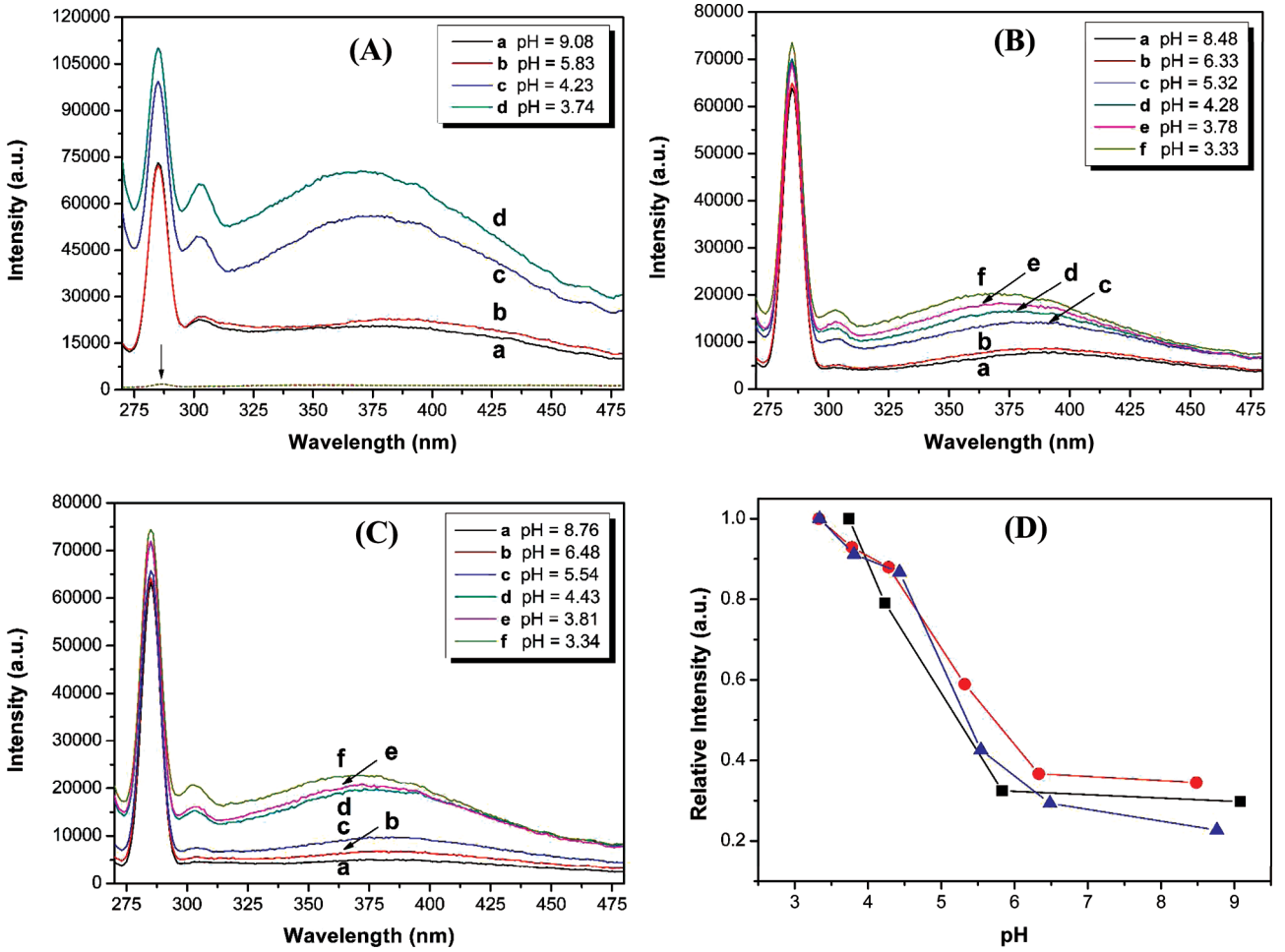

Figure 6. PL spectra of p(NIPAM-AA-AAm)-Ag microgels (λ_{ex} = 260 nm) synthesized at 22 °C (A, ■), 38 °C (B, ●), and 43 °C (C, ▲). The PL spectra of the p(NIPAM-AA-AAm) microgels are also presented in A (dash lines), showing a weak peak at 285 nm from water Raman and not fluorescence, but no other peaks. (D) The relative intensity of the peak centered at ~370 nm as a function of the pH of the surrounding media.

Theoretical work previously demonstrated that metal surface luminescence was assigned to radiative recombination of Fermi level electrons and sp- or d-band holes. The PL of noble metals could be viewed as an excitation of electrons from occupied d bands into states above the Fermi level, then subsequent electron−phonon and hole−phonon scattering processes lead to energy loss, and finally photoluminescent recombination of an electron from an occupied sp band with the hole.[40] The same fundamental mechanism is responsible for the PL of metal nanoclusters. PL of Ag clusters has been previously observed at 400 nm, similar to the observed surface plasmon average energy for 13 nm Ag nanoclusters.[41] Furthermore, it is commonly assumed that there is no PL for large metal particles, in which rapid radiation-less processes compete effectively with radiative processes.[42] Thus, the PL bands observed in our hybrid microgels could be attributed to the small Ag NPs immobilized in the polymer networks. The strong PL signals were from the efficient coupling of incident radiation to the surface plasmon of the small Ag NPs. The excitation wavelength (260 nm) far from the plasma absorption of Ag NPs could promise such a PL coming from the electron−hole recombination but not the radiative relaxation of the surface plasmon excimer. The multiple peaks in the present PL spectra might be due to the nonuniform size of the Ag NPs as well as the special embedding medium.[36,42]

Figure 6 shows the pH-sensitive PL property of p(NIPAM-AA-AAm)-Ag hybrid microgels in the near-ultraviolet region. The intensive peak at 285 nm is from the Raman scattering of water. The decrease in the pH value of the microgel dispersions induced an increase in fluorescence intensity and a blue shift of the maximum emission wavelength for the broad peak centered at around 370 nm, while no apparent shift of the maximum emission wavelength was observed for the small peak located at 302 nm. To confirm the reversibility of the pH-induced PL change, the PL spectra of hybrid microgel dispersions were measured for three cycles with dialysis and pH adjustment. The PL spectra were reproducible after the dialysis and pH adjustment, indicating that the pH-sensitive PL property change is reversible.

To visualize the relationship between the pH-induced volume phase transitions and the enhancement of the PL intensity of the p(NIPAM-AA-AAm) microgels, we plotted the relative PL intensity as a function of pH

(40) Apell, P.; Monreal, R.; Lundqvist, S. *Phys. Scr.* **1988**, *38*, 174.
(41) Kokkinakis, Th.; Alexopoulos, K. *Phys. Rev. Lett.* **1972**, *28*, 1632.
(42) Félix, C.; Sieber, C.; Harbich, W.; Buttet, J.; Rabin, I.; Schulze, W.; Ertl, G. *Chem. Phys. Lett.* **1999**, *313*, 105.

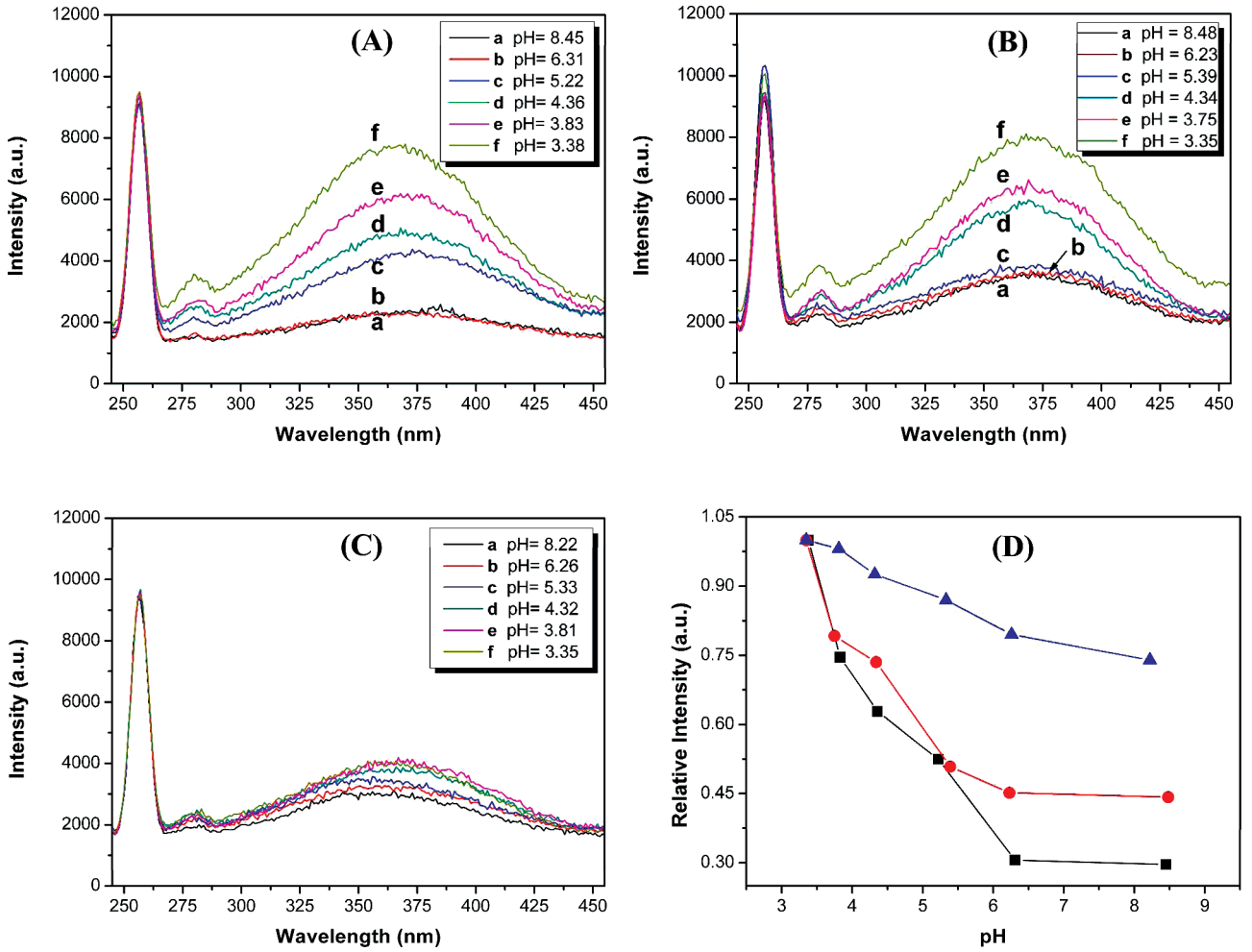

Figure 7. PL spectra of p(NIPAM-AA-AAm)-Ag/Au hybrid microgels (λ_{ex} = 236 nm) synthesized from the p(NIPAM-AA-AAm)-Ag hybrid microgel template prepared at 22 °C (A, ■), 38 °C (B, ●), and 43 °C (C, ▲). (D) The relative intensity of the peak centered at ~370 nm as a function of the pH of the surrounding media.

(Figure 6D). The comparison of Figure 2 with Figure 6D indicated that a conspicuous fluorescence increase occurred at nearly the same pH when the microgels began to shrink. The following two factors may mainly account for the pH-sensitive PL property change: (1) the change of the bonding interaction between the ligand molecules with the Ag surface and (2) the nonradiative energy loss paths. It is well-known that the optical property of a material is closely associated with its electronic structure. When a strong chemical bond is formed, it will not only change the electronic structure of the adsorbate itself but also influence to some extent the surface electronic structure of Ag crystals. This may cause a change of the local optical electric field at the metal surface.[43] The increment of the PL emission and the blue shift of the emission maximum of the p(NIPAM-AA-AAm)-Ag microgels might be resulted from the Ag−N bond's electron donation to the Ag NPs, which is similar to the Ag−S-induced blue shifts.[44] The pH-induced swelling/deswelling of the polymer network can lead to the change in the Ag−N bonding interactions because the Ag−N bonds will be stretched when the microgels swell at high pH values and compressed when the microgels collapse at low pH values. Moreover, it might be also related to the change in the number of carboxyl groups bonding with the Ag particles at different pH values, which could provoke a modification of the fluorescence properties.[11,45] On the other hand, we believe that the different nonradiative energy loss paths, related to the reduction of the number of surface defects, provide the second scenario for the PL enhancement during the microgel shrinking. The nonradiative energy loss paths are highly dependent on the nature of the environment around the metal particles.[46] In the swollen state at pH > 5.5, the ionized polymer chain tended to expand. However, the cross-linkage of the polymer chains hindered the volume expansion at a high swelling state, creating elastic tensions localized at the cross-linking points. Because of the bonding between the polymer and Ag NPs, the Ag NPs could also act as cross-linking points, introducing

(43) Kreibig, U.; Vollmer, M. Optical Properties of Metal Clusters; Springer: Berlin, 1995.
(44) (a) Malinsky, M. D.; Kelly, K. L.; Schatz, G. C.; Van Duyne, R. P. *J. Am. Chem. Soc.* **2001**, *123*, 1471. (b) Huang, T.; Murray, R. W. *J. Phys. Chem. B* **2003**, *107*, 7434.
(45) (a) Gao, M.; Kirstein, S.; Möhwald, H.; Rogach, A. L.; Kornowski, A.; Eychmüller, A.; Weller, H. *J. Phys. Chem. B* **1998**, *102*, 8360. (b) Zhang, Z.; Zhow, Z.; Yang, B.; Gao, M. *J. Phys. Chem. B* **2003**, *107*, 8.
(46) Wilcoxon, J. P.; Martin, J. E.; Parsapour, F.; Wiedenman, B.; Kelley, D. F. *J. Chem. Phys.* **1998**, *108*, 9137.

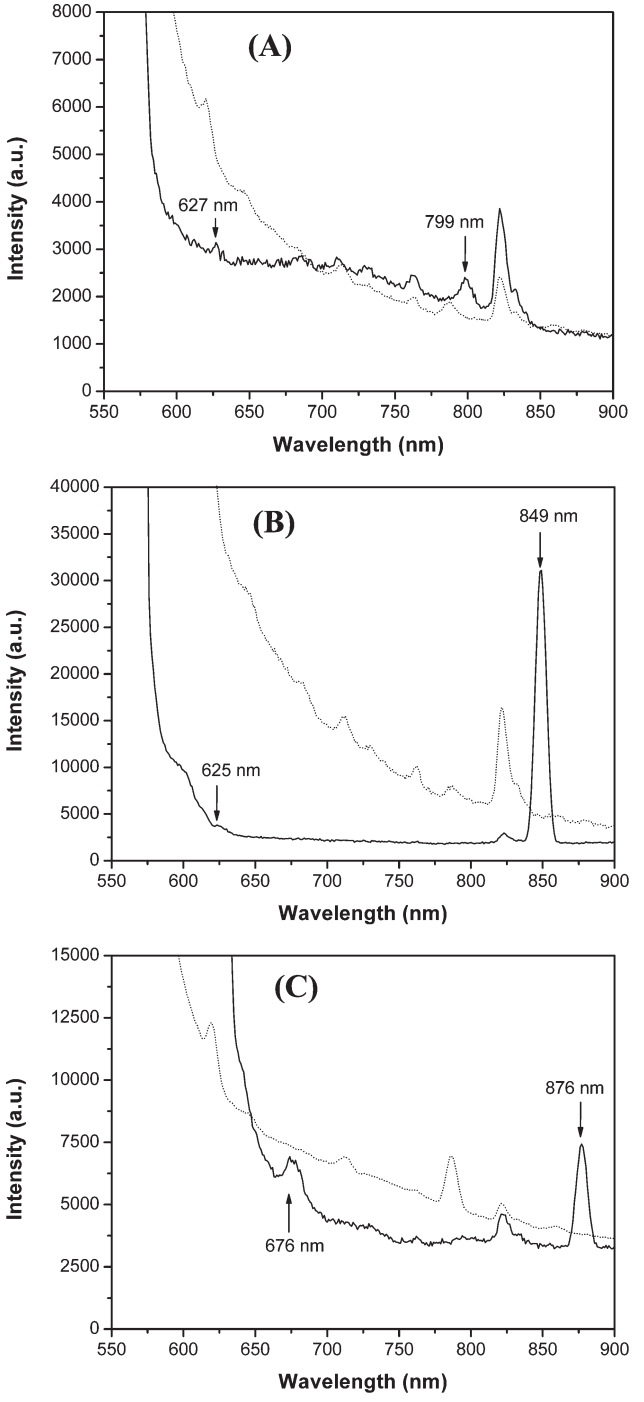

Figure 8. PL spectra of p(NIPAM-AA-AAm)-Ag/Au hybrid microgels synthesized from the p(NIPAM-AA-AAm)-Ag hybrid microgels prepared at 22 °C (A with λ_{ex} = 533 nm), 38 °C (B with λ_{ex} = 565 nm), and 43 °C (C with λ_{ex} = 585 nm). The PL spectra of corresponding p (NIPAM-AA-AAm)-Ag hybrid microgels are also presented (dashed lines) to show the difference.

an elastic tension in the bond that could stretch the polymer/Ag interface and creating surface states that could quench the PL. At lower pH values, the polymer chains are less soluble, diminishing the elastic tension and consequently reducing the number of surface trap states acting as emission quenching centers. This phenomenon is similar to the PL temperature antiquenching effect reported recently.[47] The freezing of the solvent (water) induces strain in the capping shell, and the short stabilizer molecules (2-mercaptoethanolamine) propagate the strain to the surface of the nanocrystals, creating surface quenching states.

Figure 7 shows the PL spectra of the p(NIPAM-AA-AAm)-Ag/Au hybrid microgels in the near-ultraviolet region. In comparison with the PL profiles of p(NIPAM-AA-AAm)-Ag hybrid microgels shown in Figure 6, we found that the PL profile of Ag NPs was identical, except that the effective excitation occurred at a slightly higher energy (λ_{ex} = 236 nm). After a surface modification of Ag NPs with Au clusters in the interior of the microgels, the pH-induced collapse of the microgels could still trigger the PL enhancement of the bimetallic Ag/Au NPs. However, the pH sensitivity of the PL intensity enhancement depended on the p(NIPAM-AA-AAm)-Ag hybrid microgel templates synthesized at different temperatures (Figure 7D). The Ag NPs in the interior of the p(NIPAM-AA-AAm)-Ag microgels synthesized at 22 °C have a large size. In such a system, the surface modification of the Ag NPs with Au clusters might only occur at the very superficial surface so that the total pH-induced PL enhancement (70%) is similar to that of Ag NPs without modification. When the size of Ag NPs became smaller in the p(NIPAM-AA-AAm)-Ag microgels synthesized at 38 and 43 °C, the replacement reaction of the Ag NPs with $AuCl_4^-$ could produce a deeper modification of the surface of Ag NPs. The relative high degree of surface modification of the Ag NPs with Au clusters resulted in a less pH-sensitive PL enhancement. For example, when the pH was decreased from 6.2 to 3.3, only 55% and 24% of PL intensity increase were observed for the p(NIPAM-AA-AAm)-Ag/Au hybrid microgels prepared from the p(NIPAM-AA-AAm)-Ag microgel templates synthesized at 38 and 43 °C, respectively. We therefore present a series of novel hybrid microgels with not only the reversible pH-sensitive PL property change but also the tunable pH-sensitive degree of the PL property change through the surface modification of the immobilized Ag NPs. Such well-defined tunable pH-sensitive emission confirmed that the energy states involved in nanocluster/particle luminescence are indeed perturbed by the proximity to the surface and the chemical characteristics of that surface.

Figure 8 shows the PL spectra of the p(NIPAM-AA-AAm)-Ag/Au hybrid microgels dispersed in water (pH ~ 6.1) in the visible/near-IR wavelength range obtained with excitation wavelength $\lambda_{ex} \geq 533$ nm. The PL spectra of the corresponding p(NIPAM-AA-AAm)-Ag hybrid microgels obtained under the same conditions were also presented. As expected, in addition to the PL peaks from Ag NPs, the new PL signals from Au clusters were also observed. Au clusters of different sizes produced varying amounts of PL with only the small-sized nanoclusters (< 15 nm) showing significant PL.[46] As predicted by the spherical Jellium model, the dependence of emission energy on the number of atoms, *N*, in each Au nanocluster could be

(47) Wuister, S. R.; Donegá, C. M.; Meijerink, A. *J. Am. Chem. Soc.* **2004**, *126*, 10397.

quantitatively fit for the small nanoclusters by the simple scaling relation of $E_{Fermi}/N^{1/3}$, in which E_{Fermi} is the Fermi energy of bulk Au.[43,48] For example, the emission maxima observed at 876 nm may correspond to Au_{31}.[48a] There are, however, significant differences between the present Au/Ag bimetallic NPs in the interior of microgels and the spherical Au nanoclusters reported previously,[48] leading to the difficulty in detail assignment. Nevertheless, it is clear that the surface modification of Ag NPs with Au nanoclusters significantly enhanced the PL intensity of the hybrid microgels in the near-infrared wavelength range. The strong emission in the near-infrared regime is particularly important for efficient in vivo optical imaging of biological system.[32]

Conclusions

In summary, novel hybrid microgels with Ag NPs and Ag/Au bimetallic NPs immobilized in the multiple-sensitive p(NIPAM-AA-AAm) microgels could be successfully synthesized with the pAAm as stabilizing ligands. The different swelling degrees (or mesh sizes) of the template microgels at different temperatures could be applied to control the size and size distribution of the Ag NPs formed in situ in the polymer networks. A galvanic replacement reaction could be used to modify the surface of the Ag NPs with Au nanoclusters in the interior of the microgels. The Ag NPs produced from the chemical reduction of Ag^+ ions in our p(NIPAM-AA-AAm) microgels are fluorescent. The pH-induced shrinkage of the polymer networks could modify the ligand-bonding interactions and the surface physicochemical properties of Ag NPs, resulting in a gradual increase in PL intensity and a blue shift of the emission maximum. A high degree of surface modification of the small Ag NPs with Au nanoclusters could not only tune the pH sensitivity of the PL intensity of the hybrid microgels but also significantly enhance the PL signals in the near-infrared region. These smart hybrid microgels with pH-responsive PL properties and strong PL intensity in the near-infrared regime may find important applications in biomedical and electronic devices.

Acknowledgment. We gratefully acknowledge the financial support from the National Science Foundation (CHE 0316078) and the U.S. Agency for International Development under the U.S.-Pakistan Science and Technology Cooperative Program (PGA-P280422).

(48) (a) Zhang, J.; Zhang, C. W.; Dickson, R. M. *Phys. Rev. Lett.* **2004**, *93*, 077402. (b) Bao, Y. P.; Zhong, C.; Vu, D. M.; Temirov, J. P.; Dyer, R. B.; Martinez, J. S. *J. Phys. Chem. C* **2007**, *111*, 12194.